Neutron-star crusts from the density functional theory

Nicolas Chamel
Université Libre de Bruxelles, Belgium

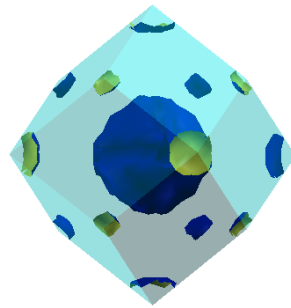

In collaboration with
S. Goriely (ULB), J. M. Pearson (UMontréal), A. F. Fantina (ULB, GANIL)
P. Haensel & J. L. Zdunik (CAMK), A. Potekhin (Ioffe)

INT, Seattle, 16 April 2018

Outline

1. Structure and equation of state of neutron-star crusts
2. Neutron superfluidity in neutron-star crusts
3. Conclusions & perspectives

Description of the outer crust of a neutron star

Main assumptions:

- **cold "catalyzed" matter** (full thermodynamic equilibrium)
  Harrison, Wakano and Wheeler, Onzième Conseil de Physique Solvay (Stoops, Brussels, Belgium, 1958) pp 124-146
- the crust is stratified into **pure layers** made of nuclei ${}^{A}_{Z}\mathrm{X}$
- electrons are $\sim$ uniformly distributed and are highly degenerate
  $T < T_{\mathrm{F}} \approx 5.93 \times 10^{9} (\gamma_r - 1)\ \mathrm{K}$

  $$\gamma_r \equiv \sqrt{1 + x_r^2}\,, \qquad x_r \equiv \frac{p_{\mathrm{F}}}{m_e c} \approx 1.00884 \left(\frac{\rho_6 Z}{A}\right)^{1/3}$$
- nuclei are arranged on a **perfect body-centered cubic lattice**

  $$T < T_m \approx 1.3 \times 10^{5} Z^2 \left(\frac{\rho_6}{A}\right)^{1/3}\ \mathrm{K} \qquad \rho_6 \equiv \rho / 10^{6}\ \mathrm{g\ cm^{-3}}$$

  Tondeur, A&A 14, 451 (1971)
  Baym, Pethick, Sutherland, ApJ 170, 299 (1971)

Experimental "determination" of the outer crust

The composition is completely determined by experimental atomic masses down to $\sim$ 200m for a 1.4$M_\odot$ neutron star with a 10 km radius

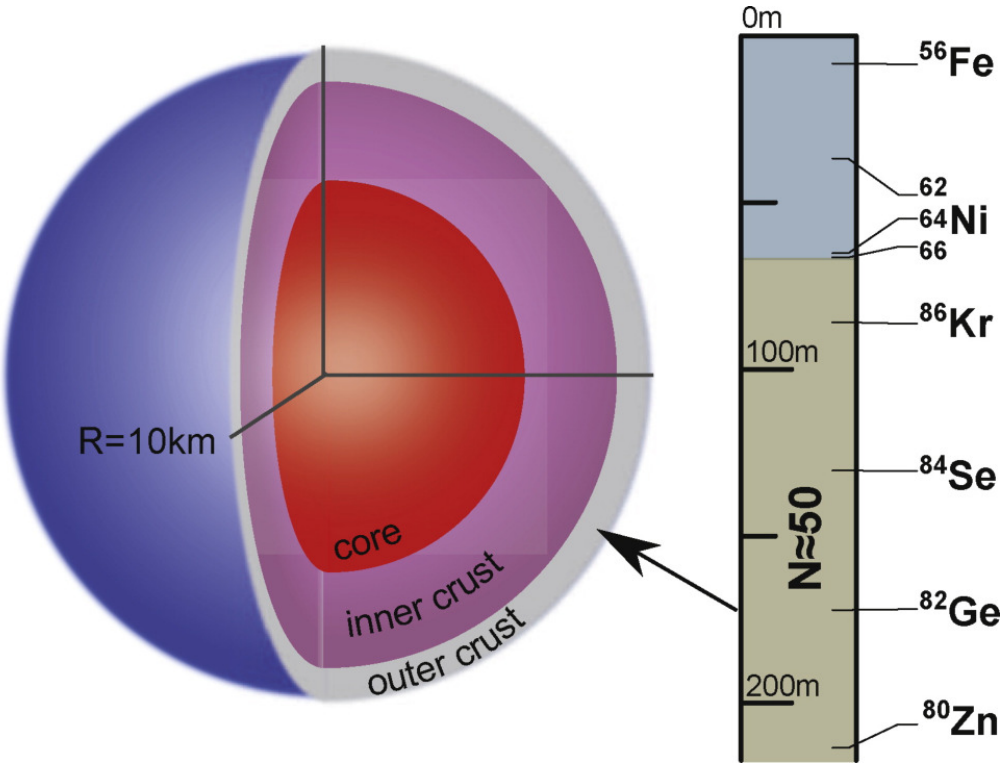

The physics governing the structure of atomic nuclei (magicity) leaves its imprint on the composition.

Due to β equilibrium and electric charge neutrality, Z is more tightly constrained than N: only a few layers with $Z = 28$.

Kreim, Hempel, Lunney, Schaffner-Bielich, Int.J.M.Spec.349-350,63(2013)

Wolf et al.,Phys.Rev.Lett.110,041101(2013)

Deeper in the star, recourse must be made to theoretical models.

Nuclear-energy density functional theory

In the **Hartree-Fock-Bogoliubov** method with (semi)local effective interactions of the Skyrme type, nucleons are described by **independent quasiparticles in self-consistent "mean" fields**:

$$\sum_{\sigma'} \begin{pmatrix} h(\boldsymbol{r})_{\sigma\sigma'} & \Delta(\boldsymbol{r})\delta_{\sigma\sigma'} \\ \Delta(\boldsymbol{r})\delta_{\sigma\sigma'} & -h(\boldsymbol{r})_{\sigma\sigma'} \end{pmatrix} \begin{pmatrix} \Psi_1(\boldsymbol{r},\sigma') \\ \Psi_2(\boldsymbol{r},\sigma') \end{pmatrix} = E \begin{pmatrix} \Psi_1(\boldsymbol{r},\sigma) \\ \Psi_2(\boldsymbol{r},\sigma) \end{pmatrix}$$

$h(\boldsymbol{r})_{\sigma'\sigma} \equiv -\boldsymbol{\nabla}\cdot B(\boldsymbol{r})\boldsymbol{\nabla}\delta_{\sigma\sigma'} + U(\boldsymbol{r})\delta_{\sigma\sigma'} - \mu\delta_{\sigma\sigma'} - \mathrm{i}\boldsymbol{W}(\boldsymbol{r})\cdot\boldsymbol{\nabla}\times\boldsymbol{\sigma}_{\sigma'\sigma}$ is the single-particle Hamiltonian,

μ is the chemical potential,

$\Delta(\boldsymbol{r})$ is the potential leading to the formation of pairs.

The HFB equations are highly nonlinear since $h(\boldsymbol{r})_{\sigma'\sigma}$ and $\Delta(\boldsymbol{r})$ are determined by the set of occupied wave functions $\{\Psi_1(\boldsymbol{r},\sigma);\Psi_2(\boldsymbol{r},\sigma)\}$.

Duguet, Lecture Notes in Physics 879 (Springer-Verlag, 2014), p. 293

Dobaczewski & Nazarewicz, in "50 years of Nuclear BCS" (World Scientific Publishing, 2013), pp.40-60

Brussels-Montreal Skyrme functionals (BSk)

For application to extreme astrophysical environments, functionals should reproduce global properties of both finite nuclei and infinite homogeneous nuclear matter.

Experimental data/constraints:

- nuclear masses (rms $\sim 0.5 - 0.6$ MeV$/c^2$)
- nuclear charge radii (rms ~ 0.03 fm)
- symmetry energy $29 \leq J \leq 32$ MeV
- incompressibility $K_v = 240 \pm 10$ MeV

Many-body calculations using realistic interactions:

- equation of state of pure neutron matter
- ${}^1S_0$ pairing gaps in nuclear matter
- effective masses in nuclear matter
- stability against spin and spin-isospin fluctuations

Chamel et al., Acta Phys. Pol. B46, 349(2015)

Neutron-matter stiffness

BSk19, BSk20 and BSk21 were fitted to realistic neutron-matter equations of state with different of degrees of stiffness:

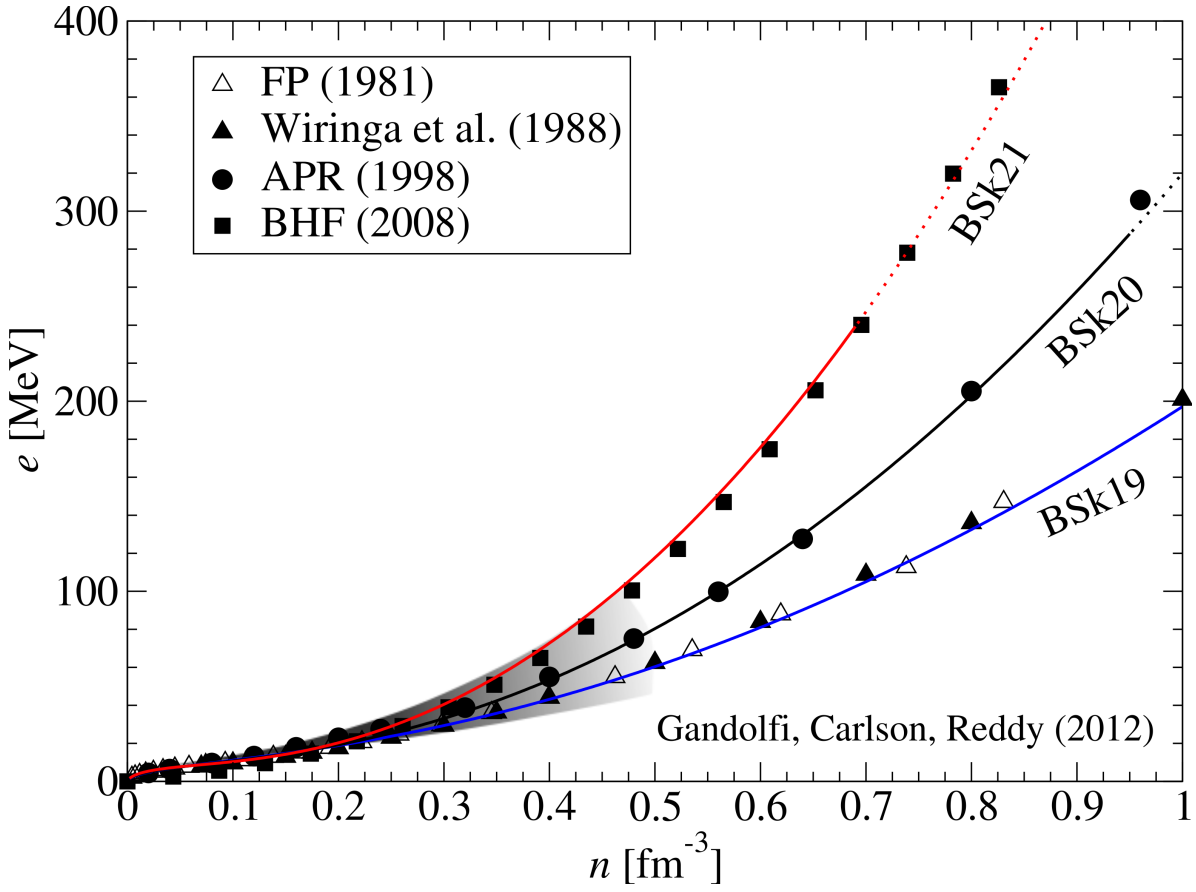

Goriely, Chamel, Pearson, Phys. Rev. C 82, 035804 (2010).

Symmetry-energy constraint

The functionals BSk22-26 were also fitted to realistic neutron-matter equations of state but with different values for $J = 29 - 32$ MeV:

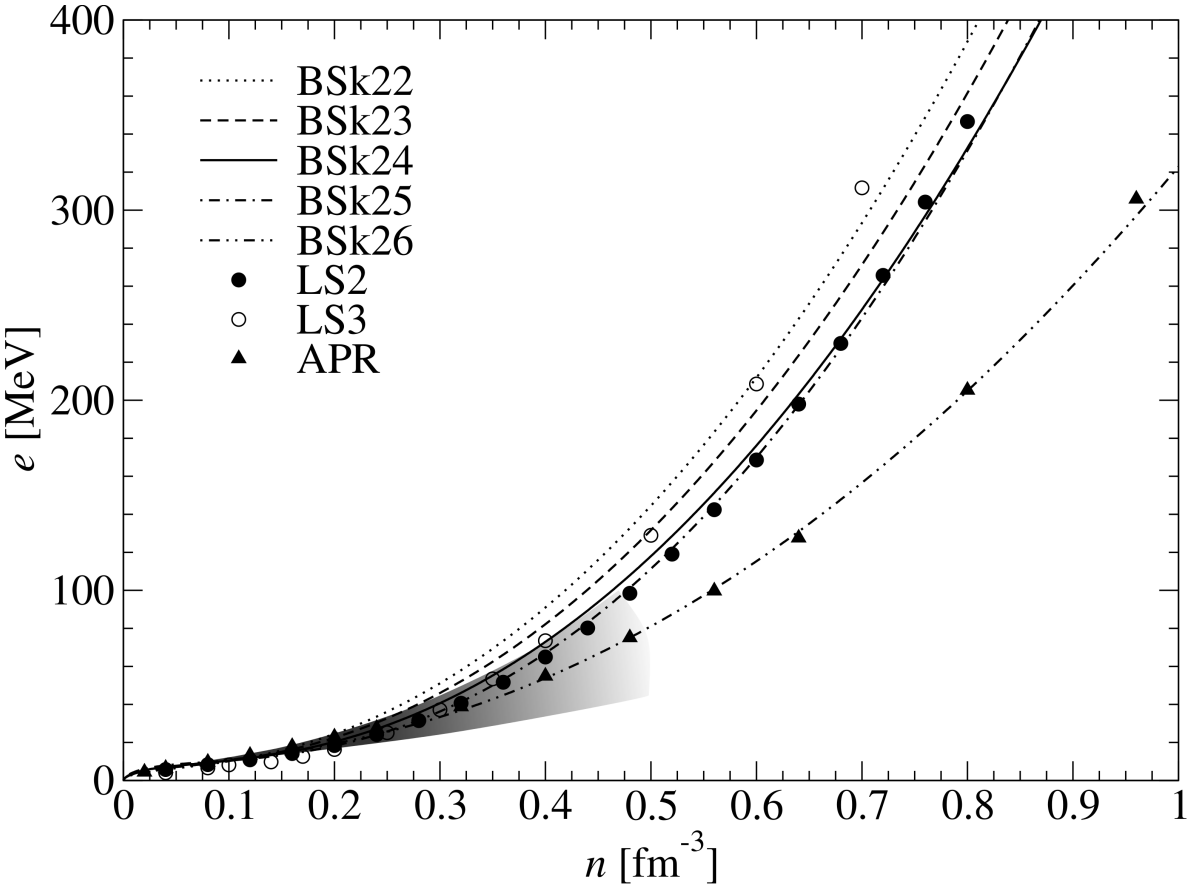

Goriely, Chamel, Pearson, Phys.Rev.C 88, 024308 (2013).

Theoretical predictions of the outer crust

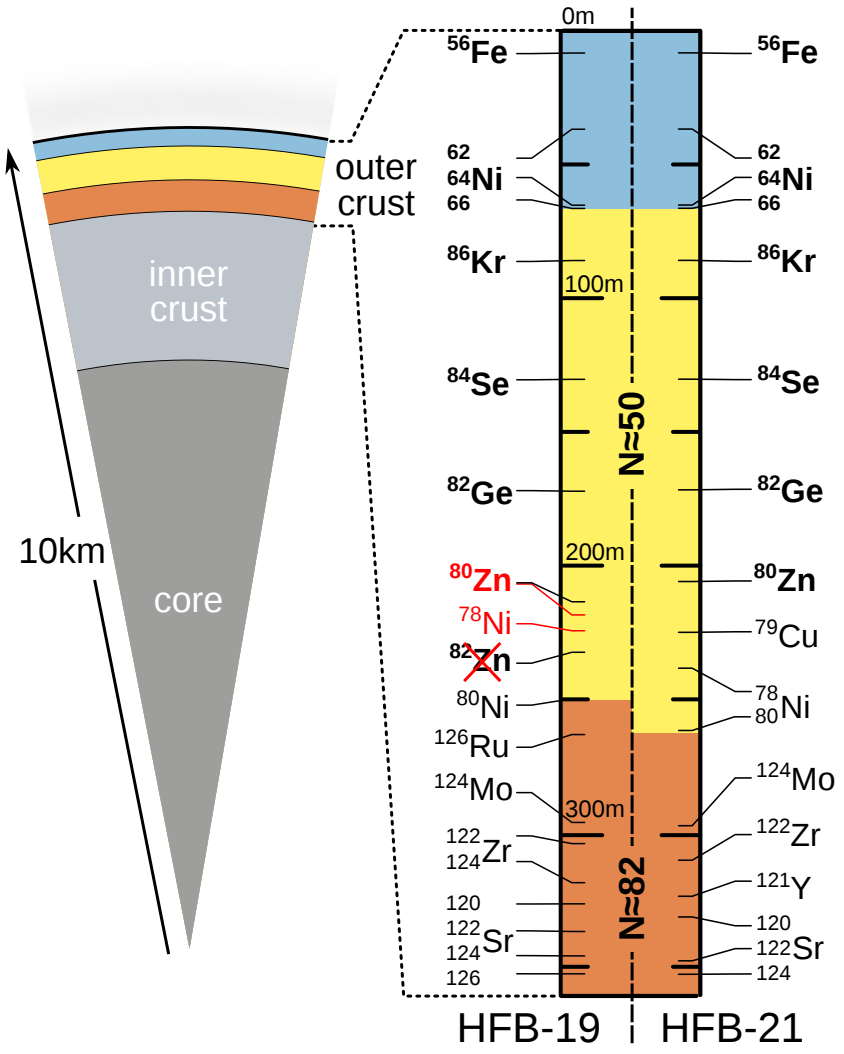

- Predictions from HFB-21 of **odd nuclei** ^{79}Cu, ^{121}Y.
- Composition dominated by nuclei with N close to **magic number** $N = 82$.
- Sr isotopes are the **most abundant** nuclides ($\sim$ 40%).

only 0.04% in Earth's crust

Pearson et al.,Phys.Rev.C83,065810(2011)

Wolf et al.,Phys.Rev.Lett.110,041101(2013)

Role of the symmetry energy

The composition of the outer crust is only slightly influenced by the density dependence of the symmetry energy $S(n)$.

The proton fraction varies roughly as $Y_p = \frac{Z}{A} \sim \frac{1}{2} - \frac{(12\pi^2(\hbar c)^3 P)^{1/4}}{8S}$

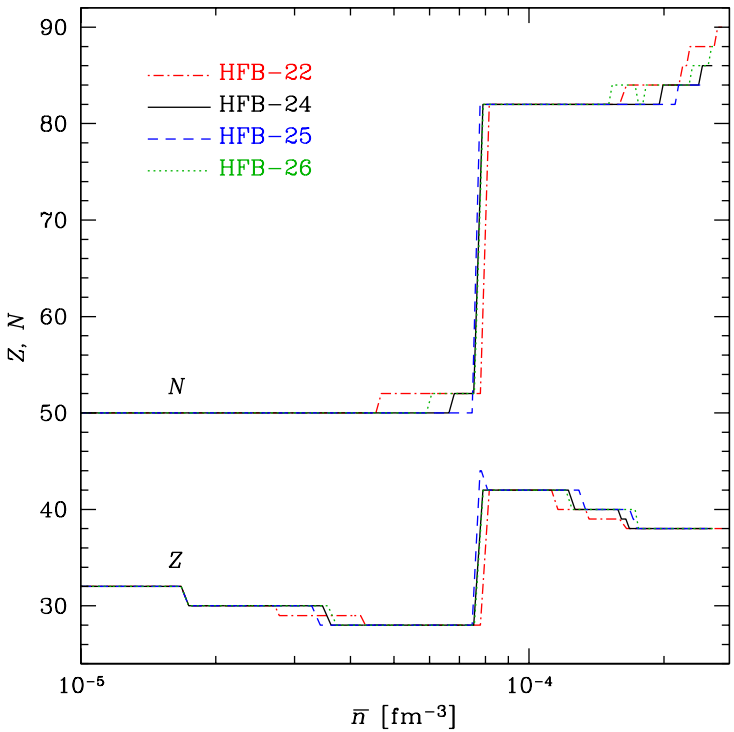

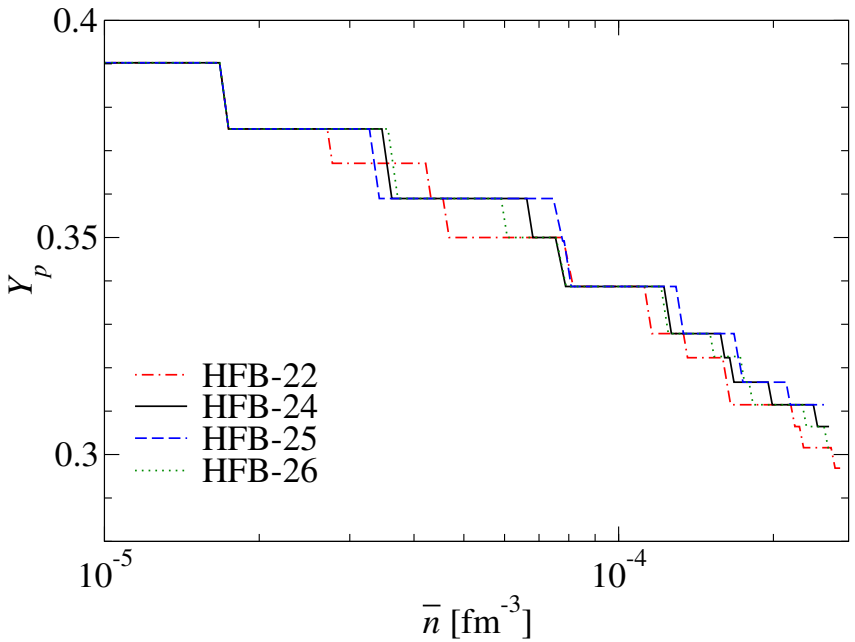

Pearson et al., Eur. Phys. J.A50,43(2014); Pearson et al. in prep.

Equation of state of the outer crust

The pressure, determined by electrons, is almost independent of the composition. Analytical fits: `http://www.ioffe.ru/astro/NSG/BSk/`

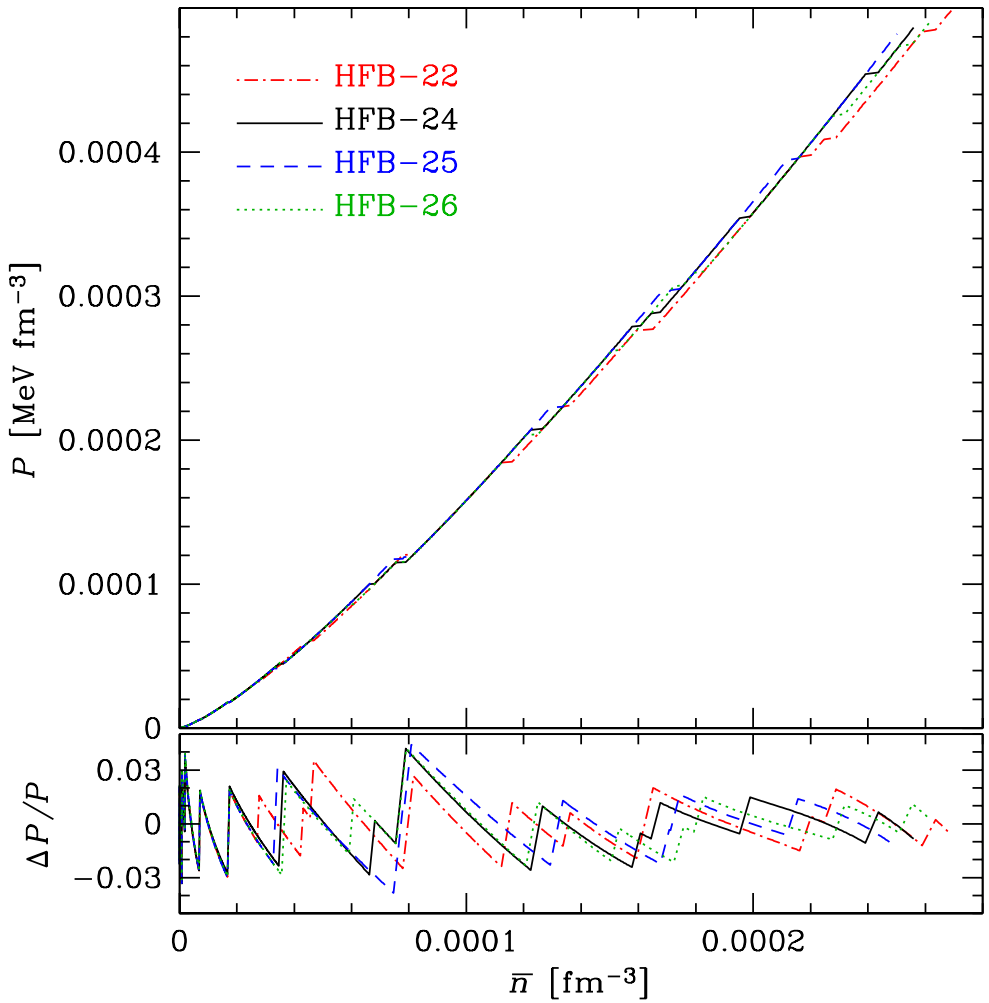

Compounds in neutron-star crusts?

Multinary ionic compounds made of nuclei with charges $\{Z_i\}$ might exist in the crust of a neutron star.

Dyson, Ann. Phys.63, 1 (1971); Witten, ApJ 188, 615 (1974)

Favorable conditions:

- **stability against weak and strong nuclear processes**.

  Jog&Smith, ApJ 253, 839(1982).

- **stability against the separation into pure (bcc) phases**:

$$\mathcal{R}(\{Z_i/Z_j\}) \equiv \frac{C}{C_{\rm bcc}} f(\{Z_i\}) \frac{\bar{Z}}{\overline{Z^{5/3}}} > 1$$

  where $f(\{Z_i\})$ is the dimensionless lattice structure function of the compound and C the corresponding structure constant.

  Chamel & Fantina, Phys. Rev. C94, 065802 (2016).

Stellar vs terrestrial compounds: (i) they are made of nuclei; (ii) electrons form an essentially uniform relativistic Fermi gas.

Substitutional compounds in neutron-star crusts

Compounds with CsCl structure are present at interfaces if $Z_1 \neq Z_2$.
But they only exist over an extremely small range of pressures.

Chamel&Fantina, Phys. Rev. C94, 065802 (2016).

Phase coexistence:

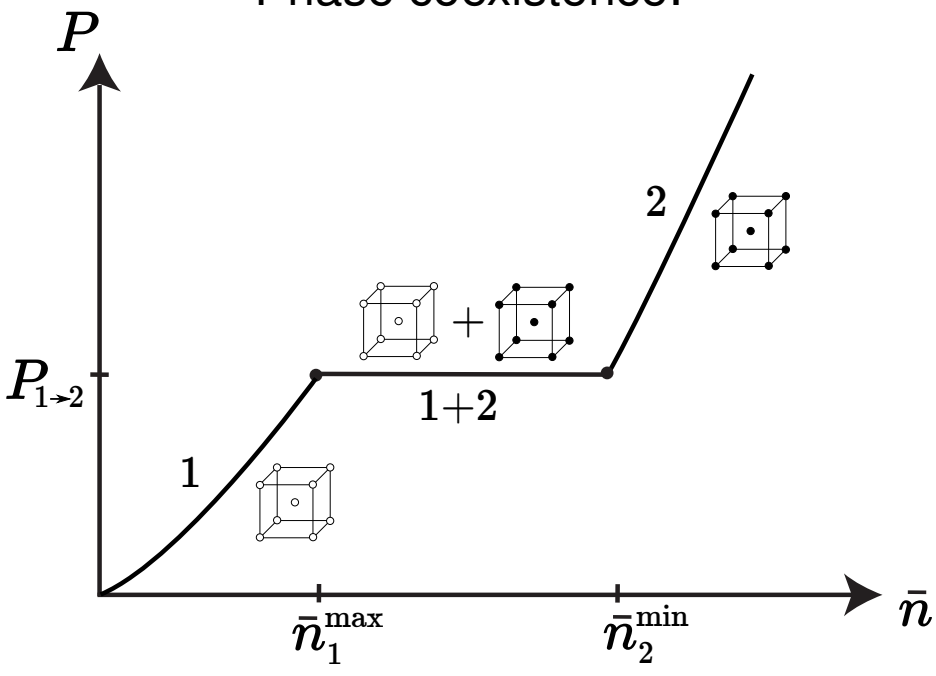

Compound:

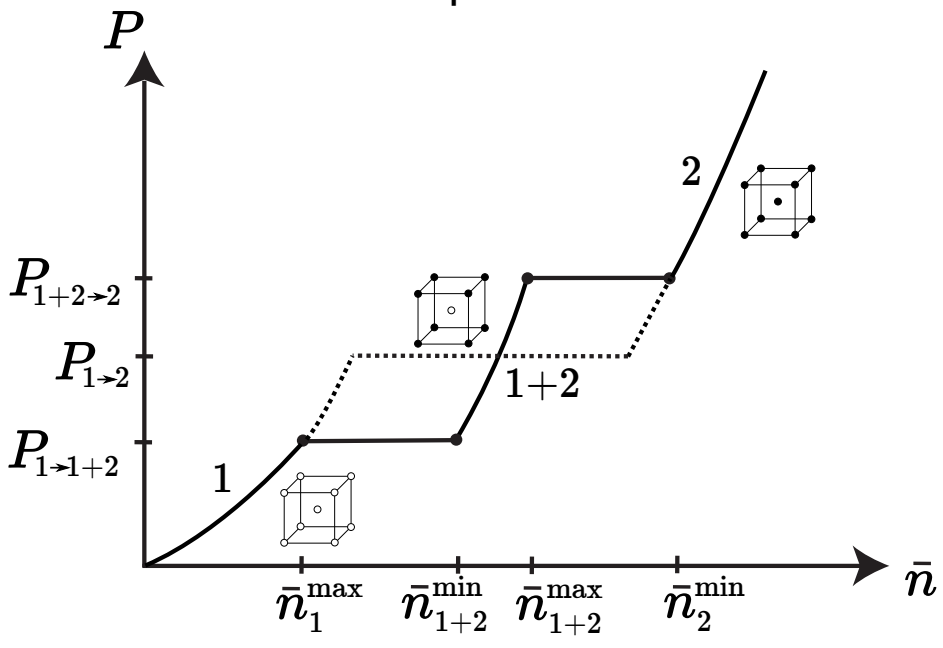

Neutron-star crust and nuclear masses

The composition of the outer crust is completely determined by **nuclear masses** $M'(A,Z)$.

Essentially **exact analytical expressions** valid for any degree of relativity of the electron gas and including electrostatic correction:
Chamel&Fantina,Phys.Rev.C94,065802(2016)

In the limit of ultrarelativistic electron Fermi gas:

$$P_{1\to 2} \approx \frac{(\mu_e^{1\to 2})^4}{12\pi^2(\hbar c)^3}, \qquad \bar{n}_1^{\max} \approx \frac{A_1}{Z_1}\frac{(\mu_e^{1\to 2})^3}{3\pi^2(\hbar c)^3}, \qquad \bar{n}_2^{\min} \approx \frac{A_2}{Z_2}\frac{Z_1}{A_1}\bar{n}_1^{\max}$$

$$\mu_e^{1\to 2} \equiv \left[\frac{M'(A_2,Z_2)c^2}{A_2} - \frac{M'(A_1,Z_1)c^2}{A_1}\right]\left(\frac{Z_1}{A_1} - \frac{Z_2}{A_2}\right)^{-1} + m_e c^2$$

Since $\bar{n}_2^{\min} > \bar{n}_1^{\max}$ in hydrostatic equilibrium, nuclei become more **neutron rich** ($Z_2/A_2 < Z_1/A_1$) and **less bound** with increasing depth.

Description of the inner crust of a neutron star

At density $\sim 4.4 \times 10^{11}$ g cm^{-3}, neutrons drip out of nuclei.

We use the 4th-order **Extended Thomas-Fermi+Strutinsky Integral (ETFSI)** approach with the *same* functional as in the outer crust:

- **semiclassical expansion in powers of** $\hbar^2$: the energy becomes a functional of $n_n(\boldsymbol{r})$ and $n_p(\boldsymbol{r})$ and their gradients only.
- **proton shell effects** are added perturbatively (neutron shell effects are much smaller and therefore neglected).

In order to further speed-up the calculations, clusters are supposed to be spherical (no pastas) and $n_n(\boldsymbol{r}), n_p(\boldsymbol{r})$ are parametrized.

Pearson,Chamel,Pastore,Goriely,Phys.Rev.C91, 018801 (2015).

Pearson,Chamel,Goriely,Ducoin,Phys.Rev.C85,065803(2012).

Onsi,Dutta,Chatri,Goriely,Chamel,Pearson, Phys.Rev.C77,065805 (2008).

The ETFSI method is a computationally very fast approximation to the full HFB equations with errors of ~ 10 keV/nucleon.

Structure of the inner crust of a neutron star

With increasing density, clusters keep $\sim$ the same size but are more and more dilute, and dissolve at $\bar{n} \sim 0.07 - 0.09$ fm^{-3}.

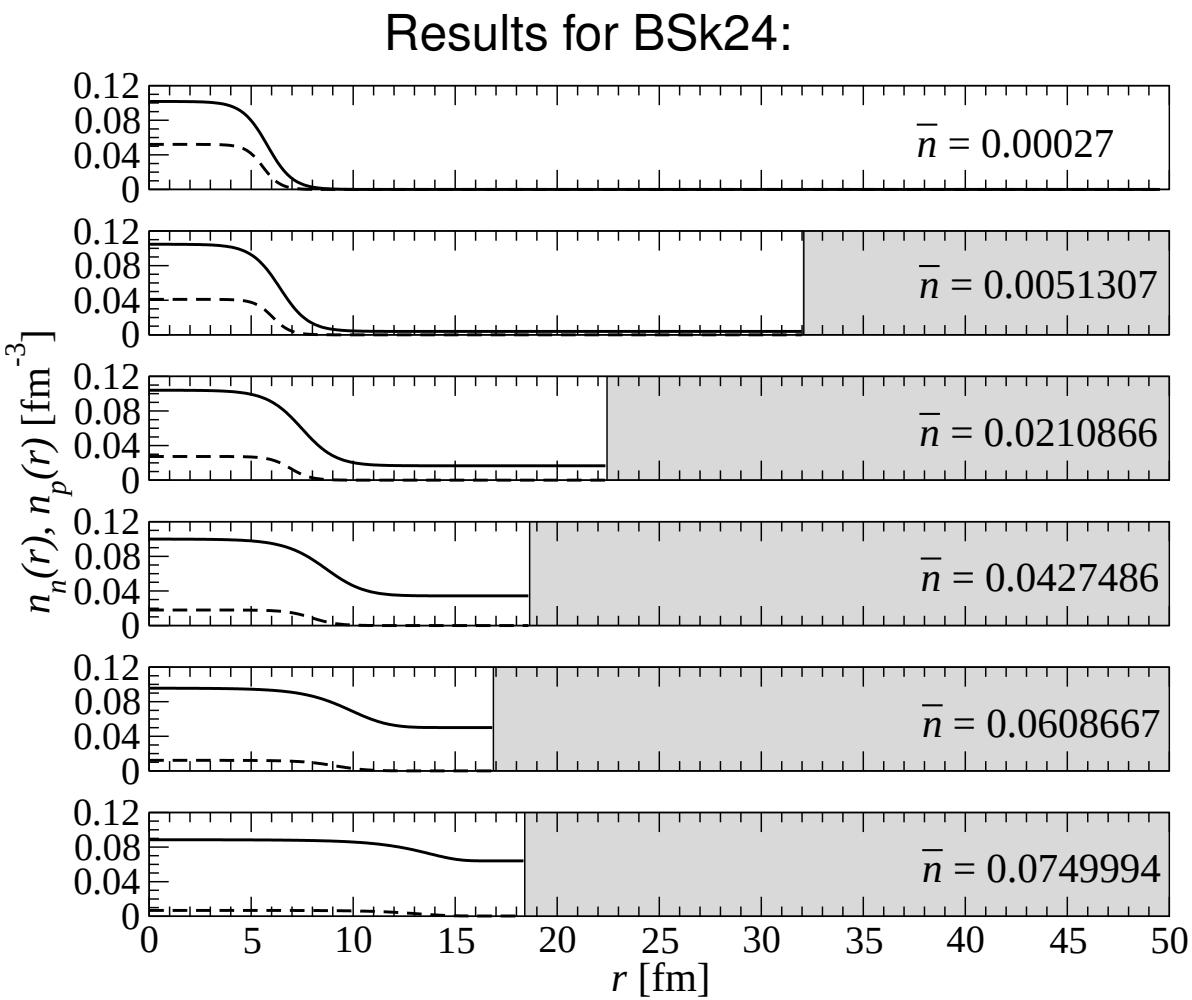

Proton shell effects in stellar environments

The ordinary nuclear shell structure is altered in dense matter: $Z = 28, 82$ disappear, while $40, 58, 92$ appear (quenched spin-orbit).

Energy per nucleon obtained with BSk24:

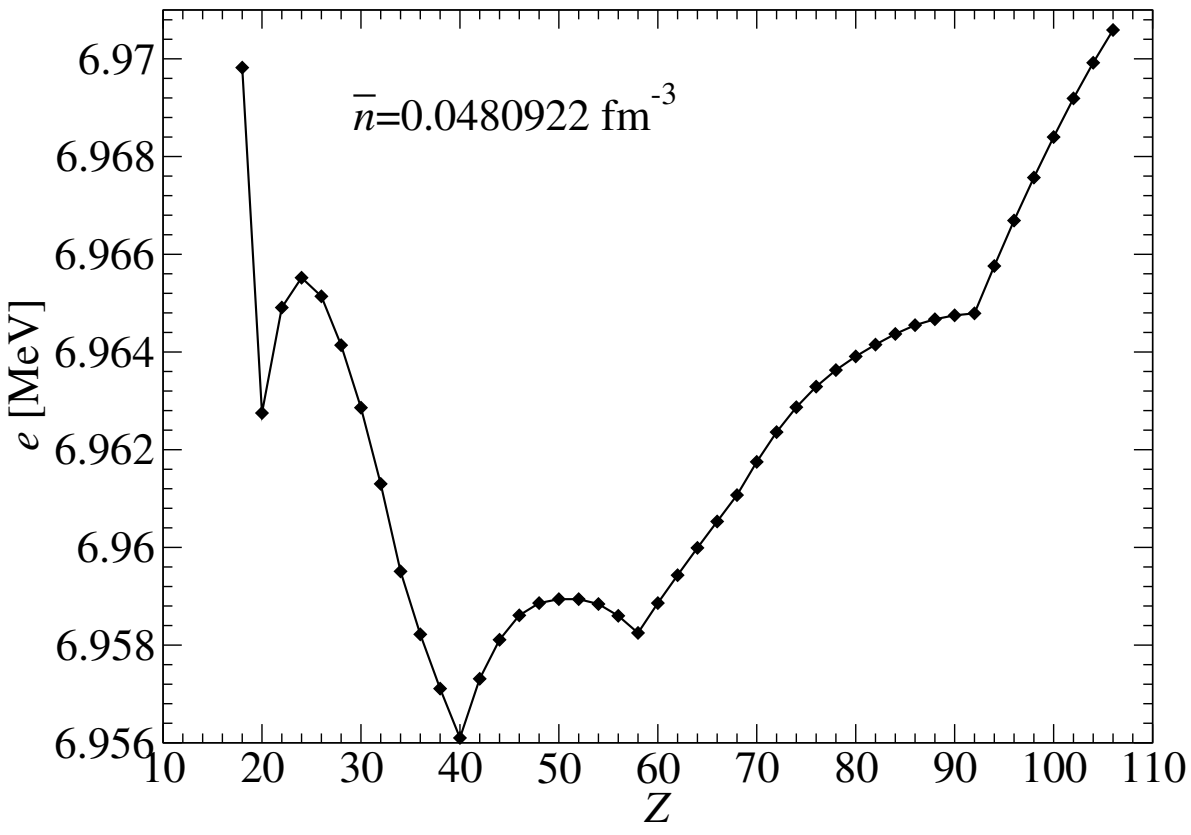

Role of shell effects and symmetry energy

The composition of the inner crust is strongly influenced by proton shell effects and the symmetry energy:

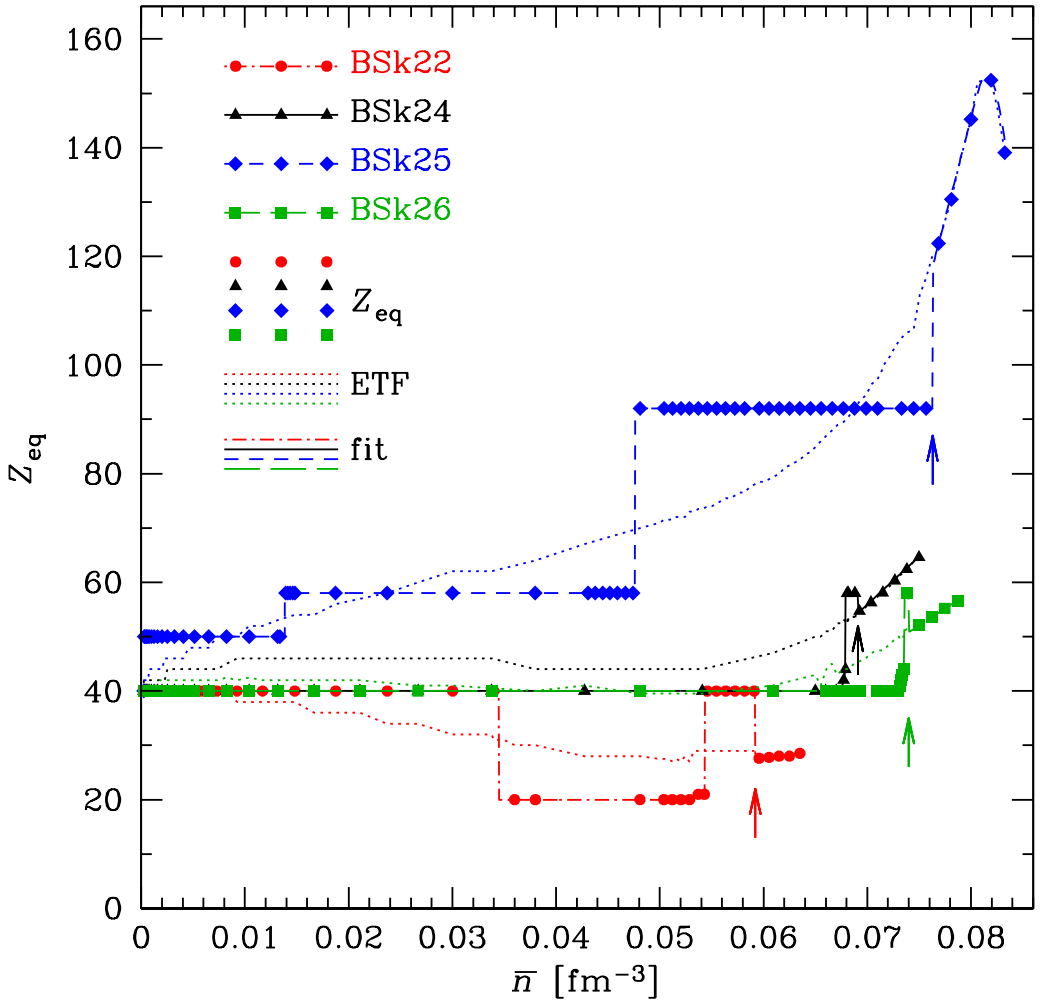

Terrestrial abundances:

Zirconium ($Z = 40$): 0.02%

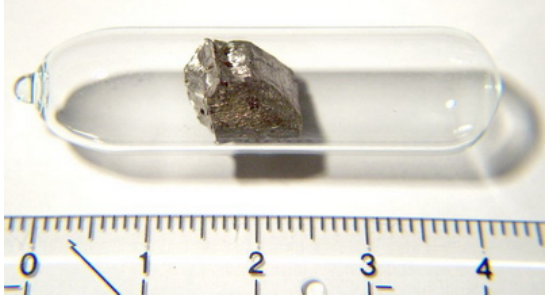

Cerium ($Z = 58$): 0.007%

Symmetry energy and proton fraction

The proton fraction Y_p of the inner crust is governed by the density dependence of the symmetry energy $S(n)$: the lower S the lower Y_p.
Analytical fits: `http://www.ioffe.ru/astro/NSG/BSk/`

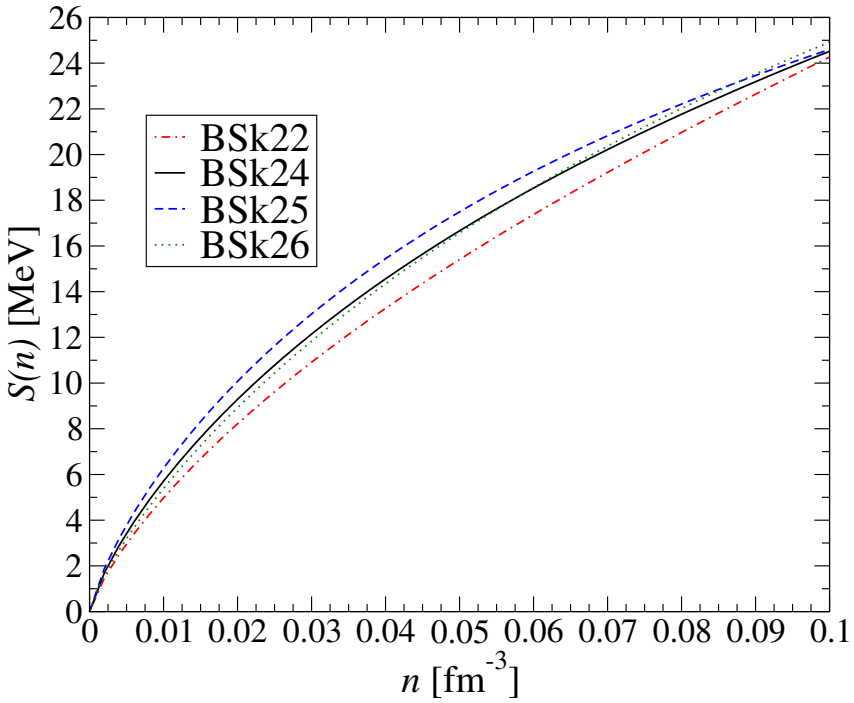

Pearson et al. in prep.

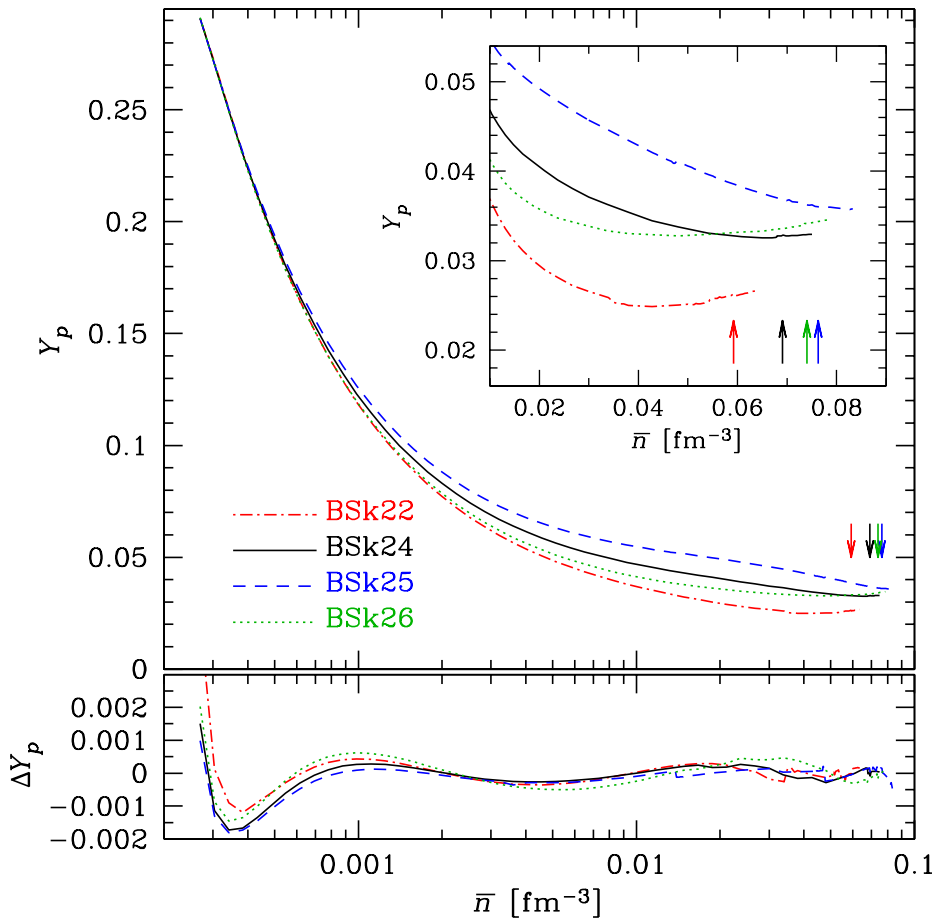

Equation of state of the inner crust

The pressure in the inner crust is related to the slope L of the symmetry energy $P \sim \frac{L}{3}\frac{n_n^2}{n_0}$

Analytical fits: `http://www.ioffe.ru/astro/NSG/BSk/`

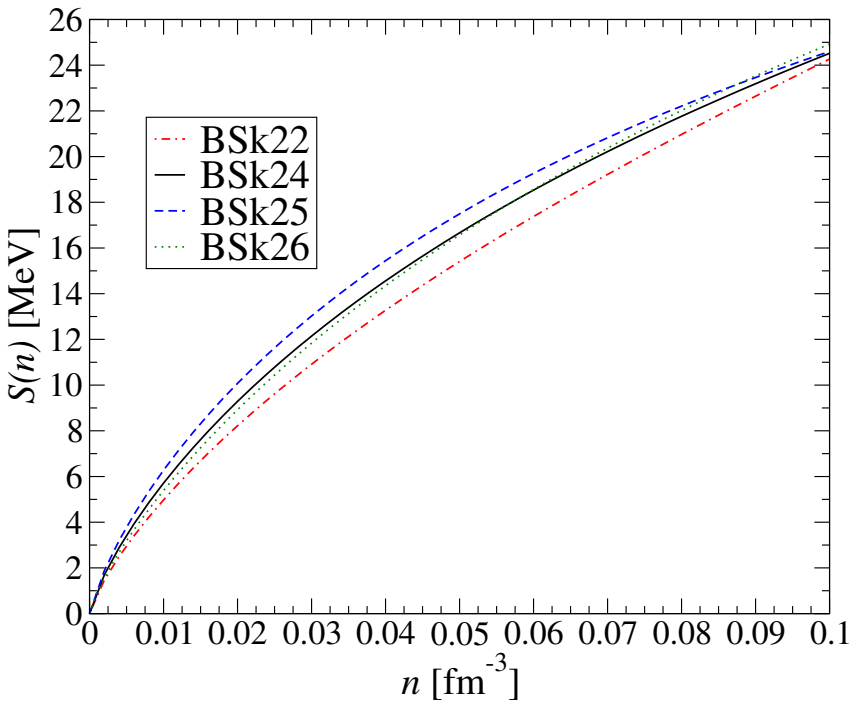

Pearson et al., in prep.

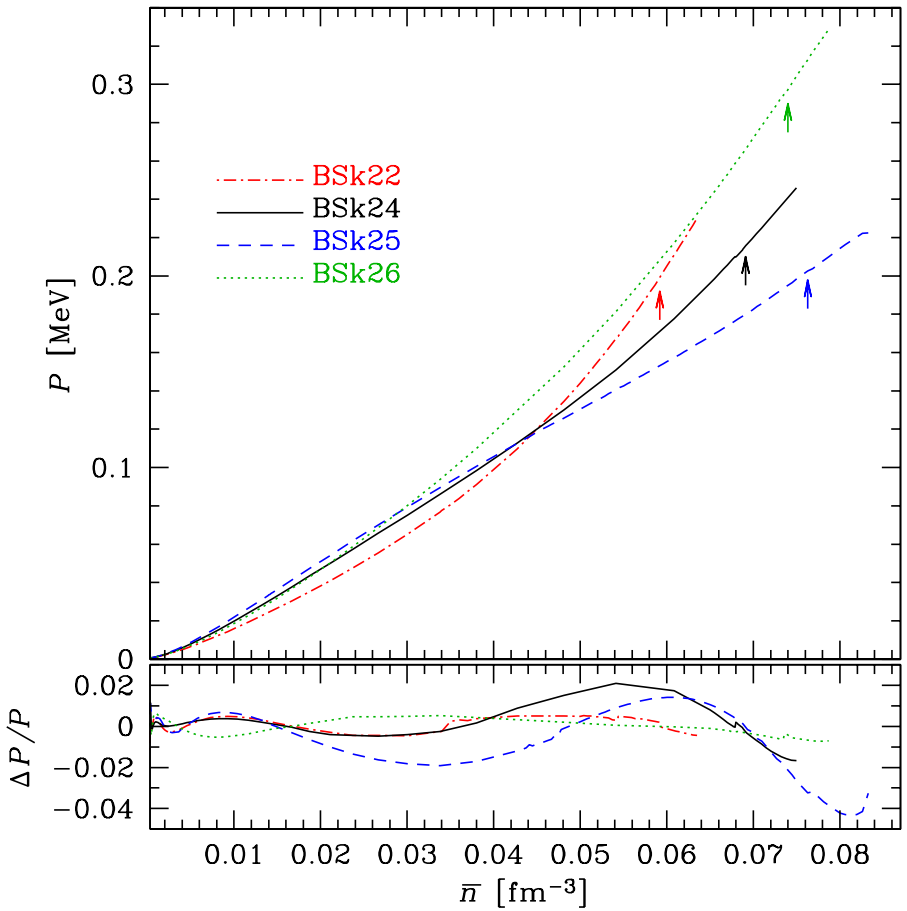

Highly-magnetized neutron stars

Some neutron stars are endowed with **extremely high surface magnetic fields** $\sim 10^{14} - 10^{15}$ G, as inferred from spin-down and spectroscopic studies.

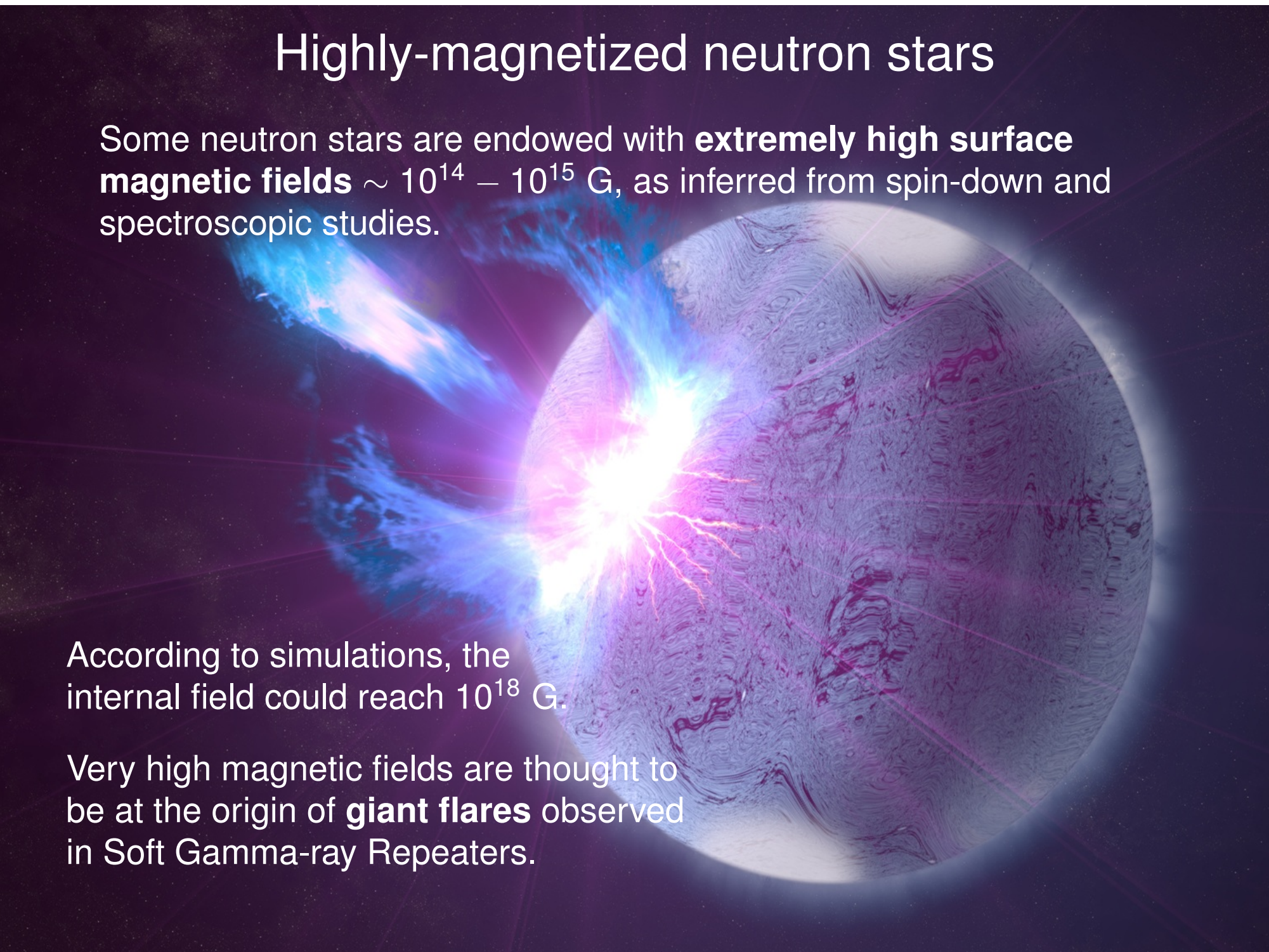

According to simulations, the internal field could reach 10^{18} G.

Very high magnetic fields are thought to be at the origin of **giant flares** observed in Soft Gamma-ray Repeaters.

Role of a high magnetic field on dense matter?

At the surface of neutron stars $B \lesssim 2 \times 10^{15}$ G.

The electron motion perpendicular to $\boldsymbol{B}$ is quantised into **Landau orbitals** with a characteristic scale $a_m = a_0\sqrt{B_{\rm at}/B}$, where a_0 is the Bohr radius

For $B \gg B_{\rm at} = m_e^2 e^3 c/\hbar^3 \simeq 2.35 \times 10^9$ G, atoms are expected to adopt a very elongated shape along $\boldsymbol{B}$ and to form **linear chains**

Ruderman, PRL27, 1306 (1971); Medin&Lai, Phys.Rev. A74, 062508 (2006)

The attractive interaction between these chains could lead to a transition into a **condensed phase** with a surface density

$$\rho_s \sim 560 A Z^{-3/5} (B/10^{12}\ {\rm G})^{6/5}\ {\rm g\ cm^{-3}}$$

In deeper regions of the crust, matter is **very stiff**

$$\rho \approx \rho_s \left(1 + \sqrt{\frac{P}{P_0}}\right), \quad P_0 \simeq 1.45 \times 10^{20} (B/10^{12}\ {\rm G})^{7/5} \left(\frac{Z}{A}\right)^2\ {\rm dyn\,cm^{-2}}$$

Lai, Rev.Mod.Phys.73, 629 (2001); Chamel et al., Phys.Rev.C86, 055804 (2012)

The intriguing case of RX J1856.5-3754

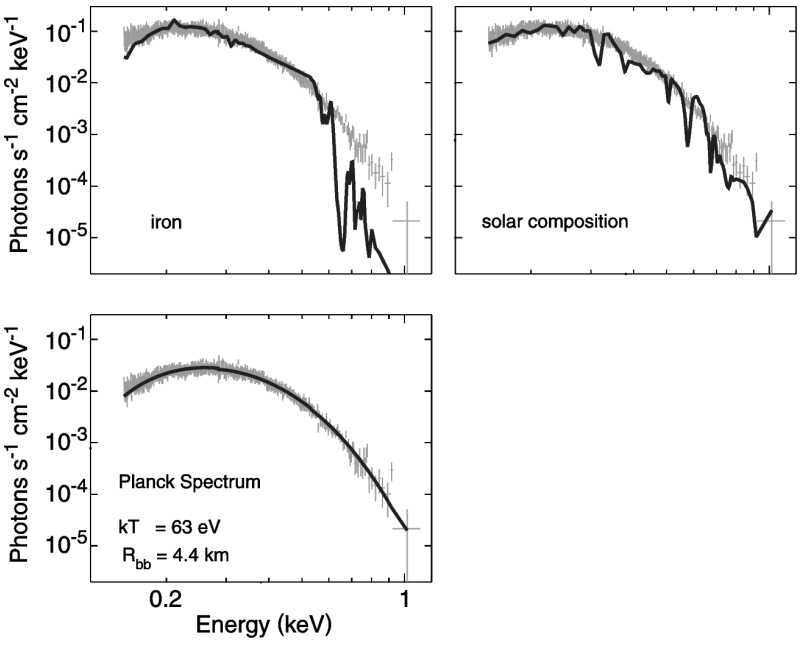

Fig. 3: The Chandra LETG X-ray spectrum of RX J1856 fitted with (non-magnetic) photospheric models assuming pure iron and solar composition. The best fit is obtained with a Planck spectrum (Burwitz et al. 2003).

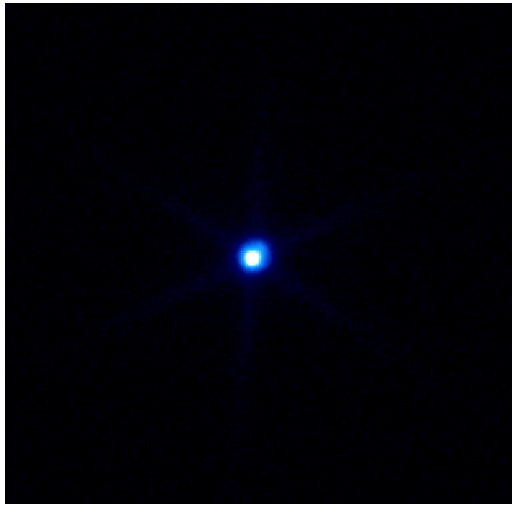

X-ray observations with Chandra

Turolla et al., ApJ 603, 265 (2004)
van Adelsberg et al., ApJ 628, 902 (2005)
Trümper (2005), astro-ph/0502457

Recent review: *Potekhin et al., Space Sci. Rev. 191, 171 (2015)*

The thermal X-ray emission is best fitted by a **black body** spectrum: evidence for a condensed surface? The presence of high ***B*** has found additional support from recent optical polarimetry measurements.
Mignani et al., MNRAS 465, 492 (2017)

Composition of highly-magnetized crust

The composition changes with B, but not the structure (bcc).

Kozhberov, Astrophys. Space Sci.361, 256 (2016)

Equilibrium nuclides for HFB-24 and $B_\star \equiv B/(4.4 \times 10^{13}\ \mathrm{G})$:

Nuclide	$B_\star$
^{58}Fe(-)	9
^{66}Ni(-)	67
^{88}Sr(+)	859
^{126}Ru(+)	1031
^{80}Ni(-)	1075
^{128}Pd(+)	1445
^{78}Ni(-)	1610
^{79}Cu(-)	1617
^{64}Ni(-)	1668
^{130}Cd(+)	1697
^{132}Sn(+)	1989

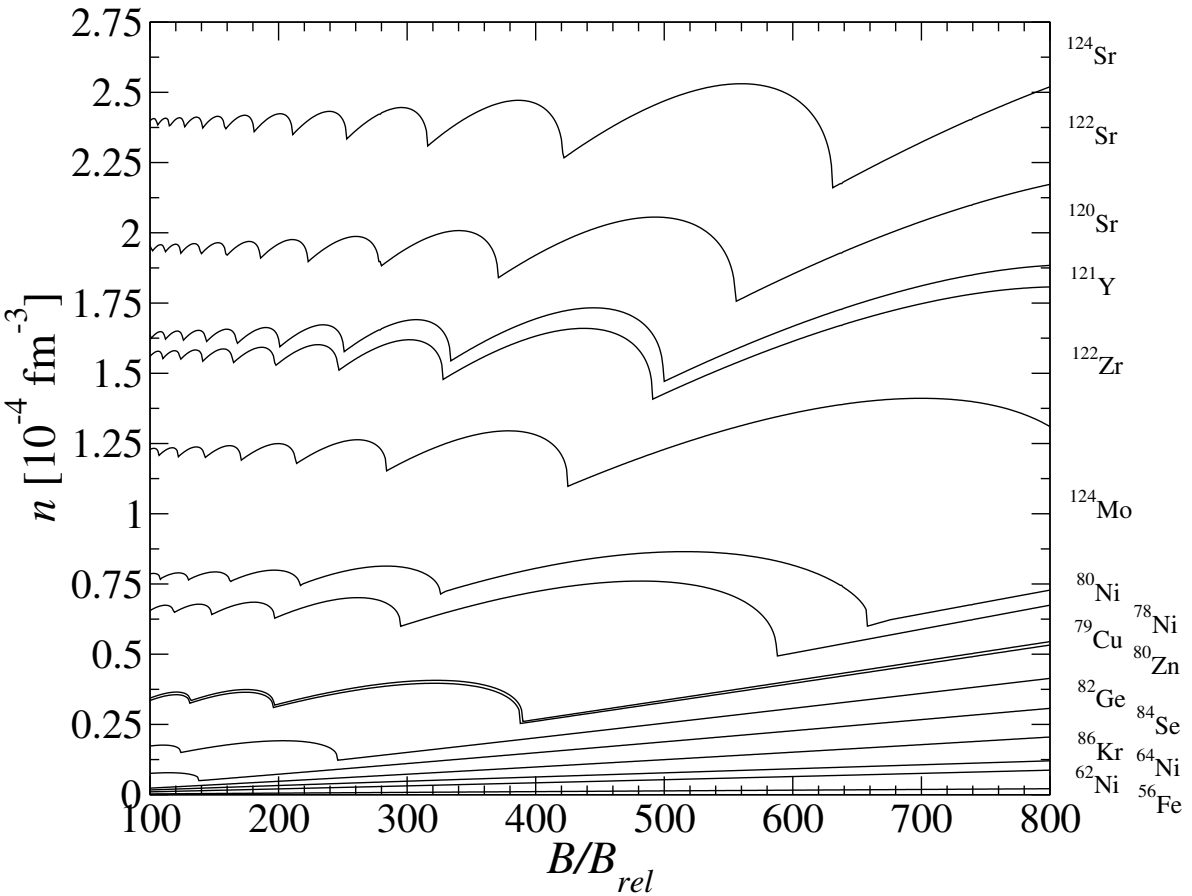

Chamel et al., Prog. Theor. Chem. & Phys. (Springer, 2017), pp 181-191.

Quantum oscillations

The neutron-drip density exhibits typical **quantum oscillations**.

Example using HFB-24:

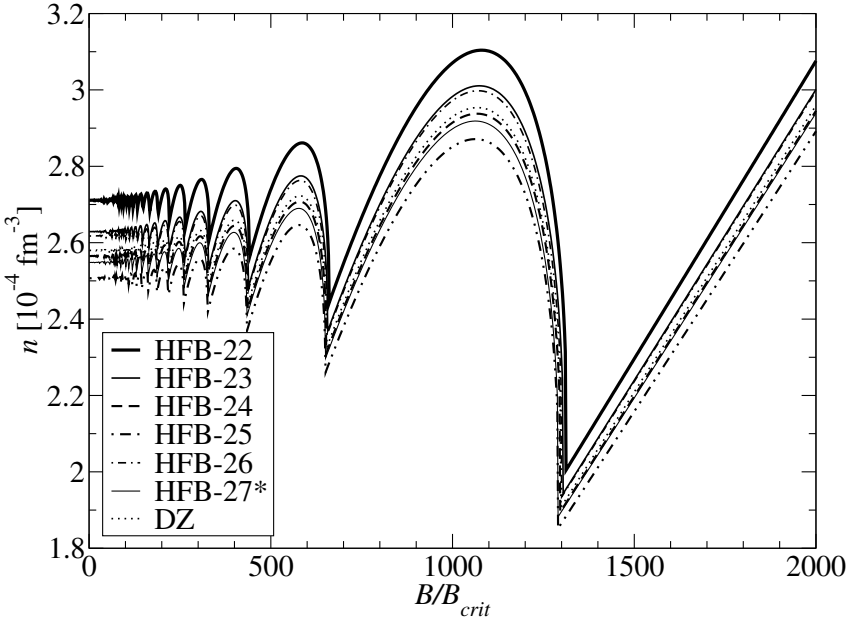

Universal oscillations:

$$\frac{\bar{n}_{\rm drip}^{\rm min}}{\bar{n}_{\rm drip}(B_\star = 0)} \approx \frac{3}{4}$$

$$\frac{\bar{n}_{\rm drip}^{\rm max}}{\bar{n}_{\rm drip}(B_\star = 0)} \approx \frac{35 + 13\sqrt{13}}{72}$$

In the strongly quantising regime,

$$\bar{n}_{\rm drip} \approx \frac{A}{Z}\frac{\mu_e^{\rm drip}}{m_e c^2}\frac{B_\star}{2\pi^2\lambda_e^3}\left[1 - \frac{4}{3}C\alpha Z^{2/3}\left(\frac{B_\star}{2\pi^2}\right)^{1/3}\left(\frac{m_e c^2}{\mu_e^{\rm drip}}\right)^{2/3}\right]$$

Chamel et al.,Phys.Rev.C91, 065801(2015).

Chamel et al.,J.Phys.:Conf.Ser.724, 012034 (2016).

Quantum oscillations

The neutron-drip density exhibits typical **quantum oscillations**.

Example using HFB-24:

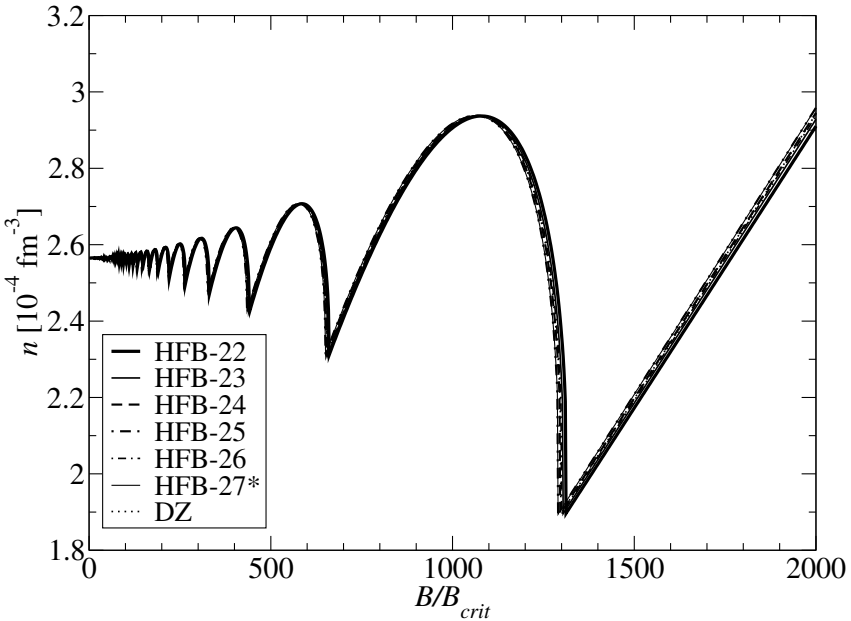

Universal oscillations:

$$\frac{\bar{n}_{\rm drip}^{\rm min}}{\bar{n}_{\rm drip}(B_\star = 0)} \approx \frac{3}{4}$$

$$\frac{\bar{n}_{\rm drip}^{\rm max}}{\bar{n}_{\rm drip}(B_\star = 0)} \approx \frac{35 + 13\sqrt{13}}{72}$$

In the strongly quantising regime,

$$\bar{n}_{\rm drip} \approx \frac{A}{Z}\frac{\mu_e^{\rm drip}}{m_e c^2}\frac{B_\star}{2\pi^2\lambda_e^3}\left[1 - \frac{4}{3}C\alpha Z^{2/3}\left(\frac{B_\star}{2\pi^2}\right)^{1/3}\left(\frac{m_e c^2}{\mu_e^{\rm drip}}\right)^{2/3}\right]$$

Chamel et al.,Phys.Rev.C91, 065801(2015).

Chamel et al.,J.Phys.:Conf.Ser.724, 012034 (2016).

Accretion and X-ray binaries

The composition of the crust may be changed by

- the **fallback** of material from the supernova explosion,
- the **accretion** of matter from a stellar companion.

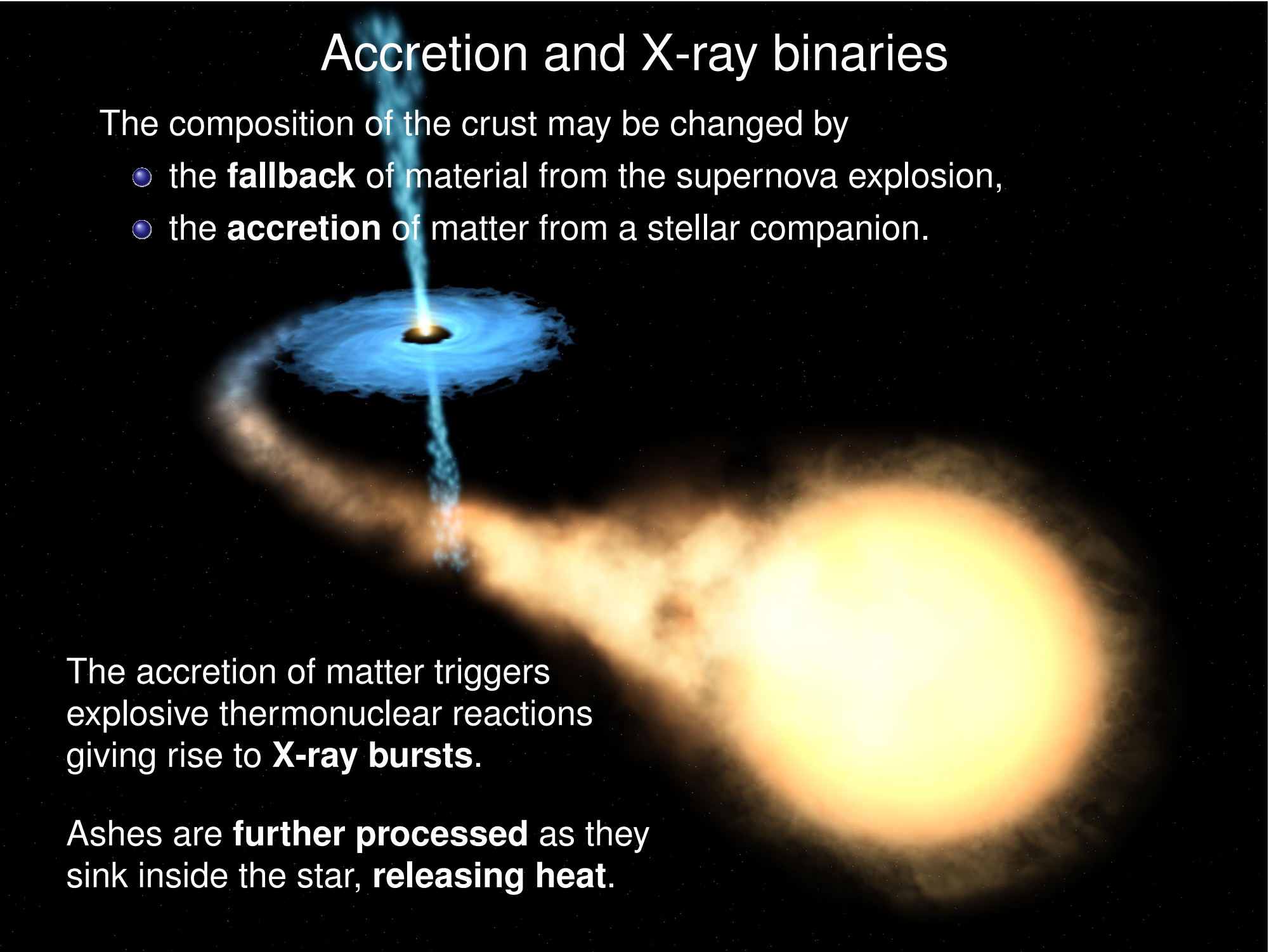

The accretion of matter triggers explosive thermonuclear reactions giving rise to **X-ray bursts**.

Ashes are **further processed** as they sink inside the star, **releasing heat**.

Accreted neutron star crusts

The original crust is buried in the core and replaced by accreted material with very different properties.

Composition and crustal heating for ashes made of ^{56}Fe:

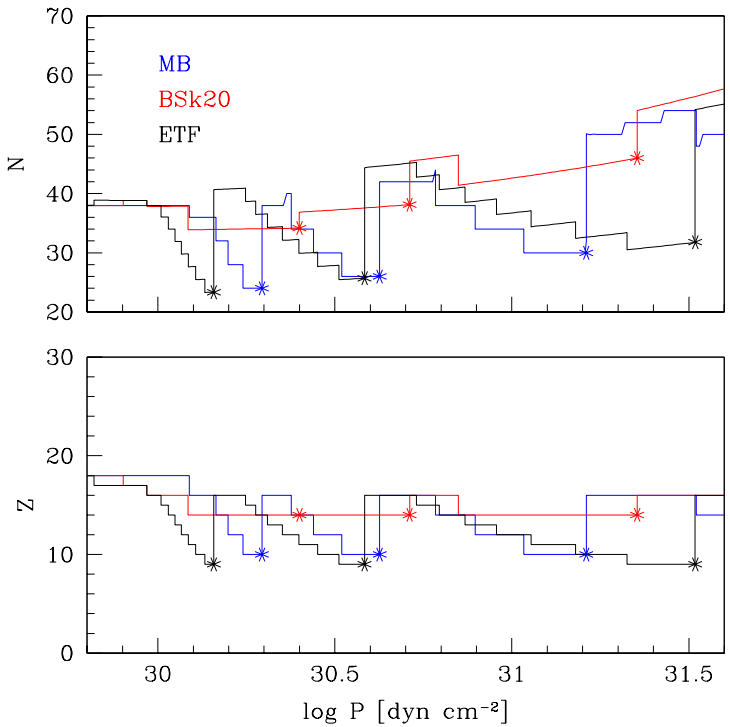

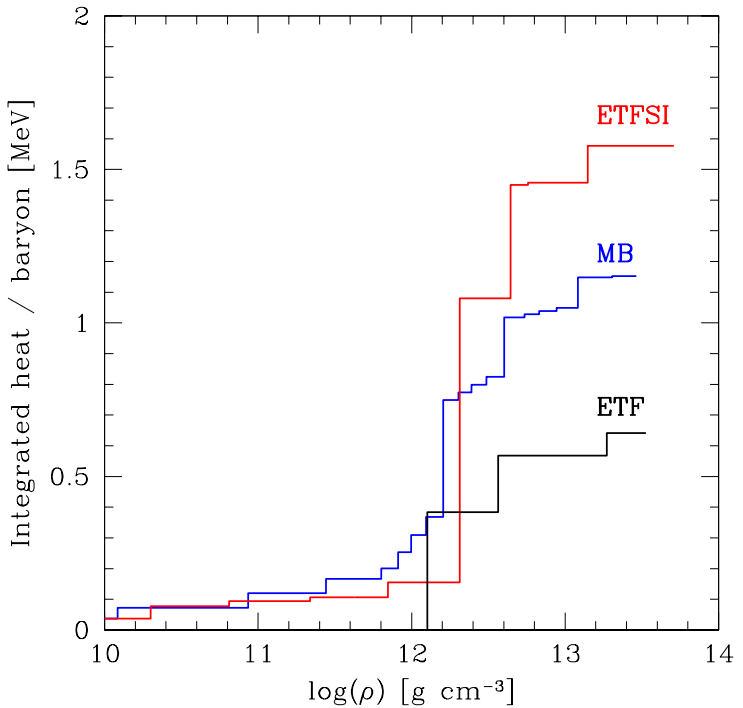

Results are very sensitive to shell effects (magic number $Z = 14$)

Fantina,Zdunik,Chamel,Pearson,Haensel,Goriely, in prep.

Compounds in accreted crusts

Various compounds can form from ashes of X-ray bursts:

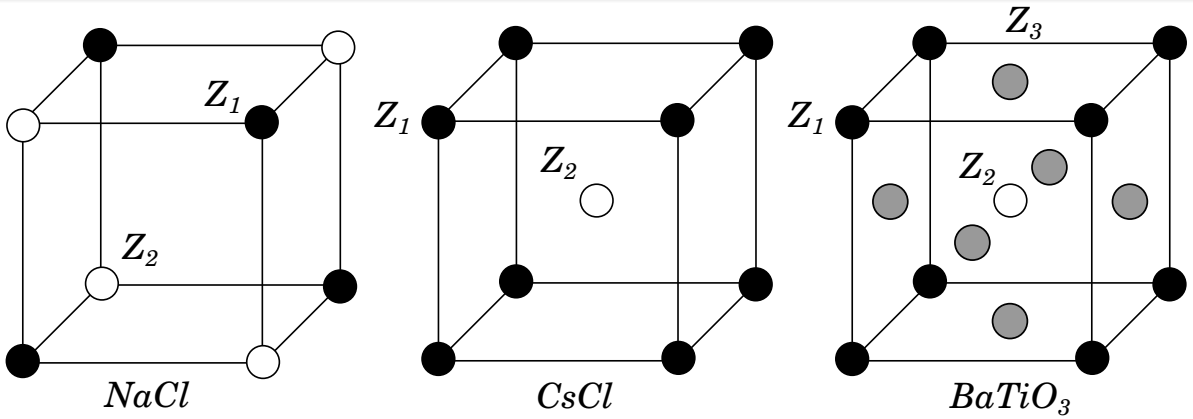

- Rocksalt: **AgNe**.
- Cesium chloride: **AgCa**, AgTi, AgCr, AgFe, **AgCo**, AgNi, AgZn, AgGe, AgAs, AgSe, **AgKr**, **KrCa**, KrTi, KrCr, KrFe, **KrCo**, KrNi, KrZn, KrGe, KrAs, KrSe, SeCa, SeTi, SeCr, SeFe, SeCo, SeNi, SeZn, SeGe, SeAs, AsCa, AsTi, AsCr, AsFe, AsCo, AsNi, AsZn, AsGe, GeCa, GeTi, GeCr, GeFe, GeCo, GeNi, GeZn, ZnCa, ZnTi, ZnCr, ZnFe, ZnCo, ZnNi, NiCa, NiTi, NiCr, NiFe, NiCo, **CoCa**, CoTi, CoCr, CoFe, FeCa, FeTi, FeCr, CrCa, **CrTi**, TiCa.
- Perovskite: $AgNeO_3$.

Chamel, J. Phys. Conf.S.932, 012039 (2017)

Superfluid flow in a periodic medium

Similarly to superfluid ^{4}He on thin films, superconducting electrons in solids, or atomic gases in optical lattices, **superfluid neutrons in neutron-star crusts do not flow freely** despite the absence of viscous drag.

The neutron current in the crust rest frame can be written as

$$\boldsymbol{j_n} = n_n^s \boldsymbol{v_n}$$

$\boldsymbol{v_n}$ is the neutron "superfluid velocity"

n_n^s is the **neutron "superfluid" or "conduction" density**

The neutron superfluid density n_n^s is generally not equal to the density n_n^f of free neutrons due to the **breaking of translational symmetry**.

Recent review:

Chamel, J. Low. Temp. Phys. 189, 328 (2017) - arXiv:1707.07854

Density functional theory in a periodic medium

Floquet-Bloch theorem

> *I found to my delight that the wave differed from the plane wave of free electrons only by a periodic modulation.*

Bloch, Physics Today 29 (1976), 23-27.

The wave functions satisfy

$$\Psi_{1\alpha\boldsymbol{k}}(\boldsymbol{r}+\boldsymbol{\ell},\sigma) = e^{\mathrm{i}\,\boldsymbol{k}\cdot\boldsymbol{\ell}}\Psi_{1\alpha\boldsymbol{k}}(\boldsymbol{r},\sigma)$$
$$\Psi_{2\alpha\boldsymbol{k}}(\boldsymbol{r}+\boldsymbol{\ell},\sigma) = e^{\mathrm{i}\,\boldsymbol{k}\cdot\boldsymbol{\ell}}\Psi_{2\alpha\boldsymbol{k}}(\boldsymbol{r},\sigma)$$

for any lattice vector $\boldsymbol{\ell}$.

- α (band index) accounts for the rotational symmetry around each lattice site,
- $\boldsymbol{k}$ (wave vector) accounts for the translational symmetry of the crystal.

Chamel, Goriely, Pearson, in "50 years of Nuclear BCS" (World Scientific Publishing, 2013), pp.284-296.

multiband BCS gap equations

Due to **proximity effects**, superfluidity permeates the clusters so that $\Delta(\boldsymbol{r})$ varies smoothly in neutron-star crusts.

In the **decoupling approximation** $\Psi_{1\alpha\boldsymbol{k}} \approx U_{\alpha\boldsymbol{k}}\varphi_{\alpha\boldsymbol{k}}, \quad \Psi_{2\alpha\boldsymbol{k}} \approx V_{\alpha\boldsymbol{k}}\varphi_{\alpha\boldsymbol{k}}$, where $\varphi_{\alpha\boldsymbol{k}}$ are single-particle wave functions

$$\sum_{\sigma'} h(\boldsymbol{r})_{\sigma\sigma'}\varphi_{\alpha\boldsymbol{k}}(\boldsymbol{r},\sigma') = \varepsilon_{\alpha\boldsymbol{k}}\varphi_{\alpha\boldsymbol{k}}(\boldsymbol{r},\sigma),$$

the HFB equations reduce to the **multiband BCS gap equations**:

$$\Delta_{\alpha\boldsymbol{k}} = -\frac{1}{2}\sum_{\beta}\int \frac{\mathrm{d}^3\boldsymbol{k'}}{(2\pi)^3}\,\bar{v}^{\mathrm{pair}}_{\alpha\boldsymbol{k}\alpha-\boldsymbol{k}\beta\boldsymbol{k'}\beta-\boldsymbol{k'}}\frac{\Delta_{\beta\boldsymbol{k'}}}{E_{\beta\boldsymbol{k'}}}$$

where $E_{\alpha\boldsymbol{k}} = \sqrt{(\varepsilon_{\alpha\boldsymbol{k}}-\mu)^2+\Delta^2_{\alpha\boldsymbol{k}}}$ and

$$U_{\alpha\boldsymbol{k}} = \frac{1}{\sqrt{2}}\sqrt{1+\frac{\varepsilon_{\alpha\boldsymbol{k}}-\mu}{E_{\alpha\boldsymbol{k}}}}, \quad V_{\alpha\boldsymbol{k}} = -\frac{1}{\sqrt{2}}\sqrt{1-\frac{\varepsilon_{\alpha\boldsymbol{k}}-\mu}{E_{\alpha\boldsymbol{k}}}}$$

Chamel et al., Phys.Rev.C81,045804 (2010).

The errors were found to be very small (a few keV per nucleon).

Pastore et al., PoS(INPC2016)145

Pairing field and local density approximation

Because pairing is highly nonlocal (coherence length $\xi \gg$ cluster size), both neutrons bound inside clusters and unbound neutrons contribute to superfluidity.

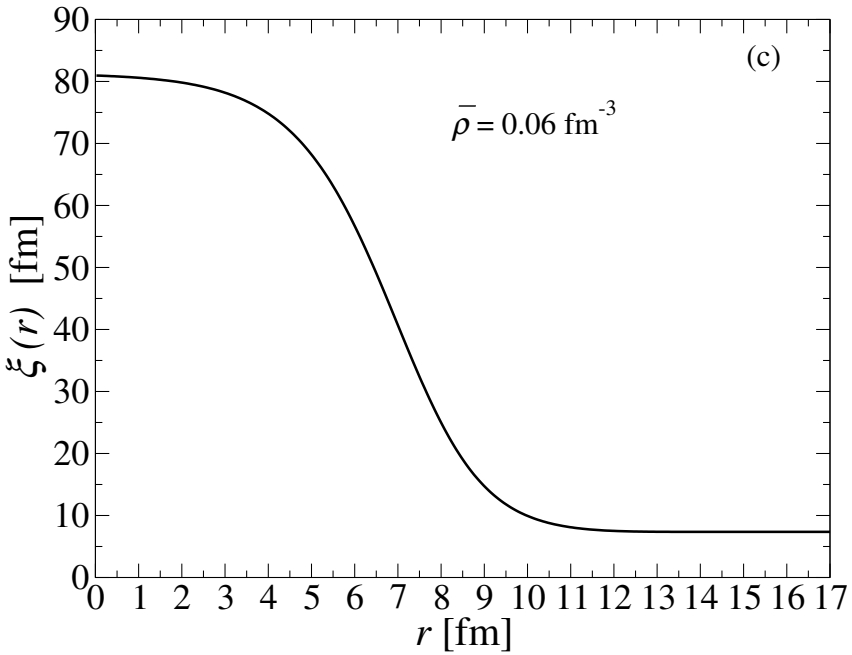

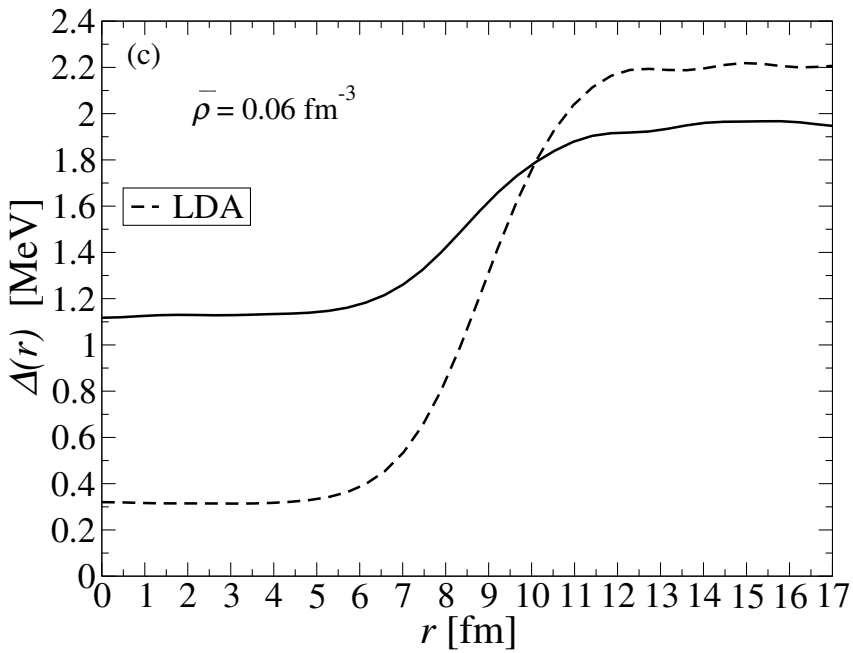

Chamel et al., Phys.Rev.C81(2010)045804.

Neutron "conduction" from the band theory

In the BCS regime, the "superfluid" neutron density is given by

$$n_n^s = \frac{m_n}{24\pi^3\hbar^2}\sum_\alpha \int |\boldsymbol{\nabla}_{\boldsymbol{k}}\varepsilon_{\alpha\boldsymbol{k}}|^2 \frac{\Delta_{\alpha\boldsymbol{k}}^2}{E_{\alpha\boldsymbol{k}}^3}\mathrm{d}^3k$$

This is a generalization of Landau's formula for a periodic medium.

In the **weak coupling** limit $\Delta_{\alpha\boldsymbol{k}}/\mu \to 0$, the superfluid density is completely determined by the shape of the Fermi surface **independently of pairing properties**:

$$n_n^s \approx \frac{m_n}{24\pi^3\hbar^2}\sum_\alpha \int_{\mathrm{F}} |\boldsymbol{\nabla}_{\boldsymbol{k}}\varepsilon_{\alpha\boldsymbol{k}}|\mathrm{d}\mathcal{S}^{(\alpha)}$$

Carter,Chamel,Haensel,Nucl.Phys.A748,675 (2005); Nucl.Phys.A759,441(2005)

Systematic band-structure calculations showed that $n_n^s \leq n_n^f$. At densities $\sim 0.02 - 0.04$ fm^{-3}, **most neutrons are entrained by the crust** and $n_n^s/n_n^f \lesssim 10\%$.

Chamel,Phys.Rev.C85,035801(2012).

Hydrodynamic approach

- **strong pairing limit** (coherence length $\ll$ cluster size)
- uniform density inside and outside clusters
- a fraction δ of neutrons in clusters are superfluid

The superfluidity density is **independent of the pairing properties**.

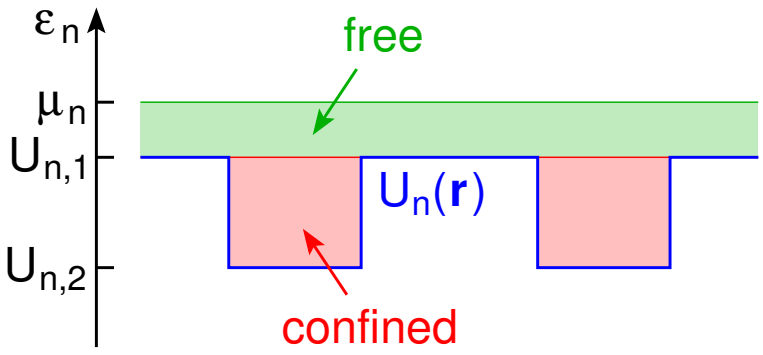

$$\frac{n_n^s}{n_n^f} \approx 1+3\frac{\mathcal{V}_{\rm I}}{\mathcal{V}_{\rm cell}}\frac{\delta-\gamma}{\delta+2\gamma}, \quad \gamma = \frac{n_n^f}{n_n^{\rm I}}$$

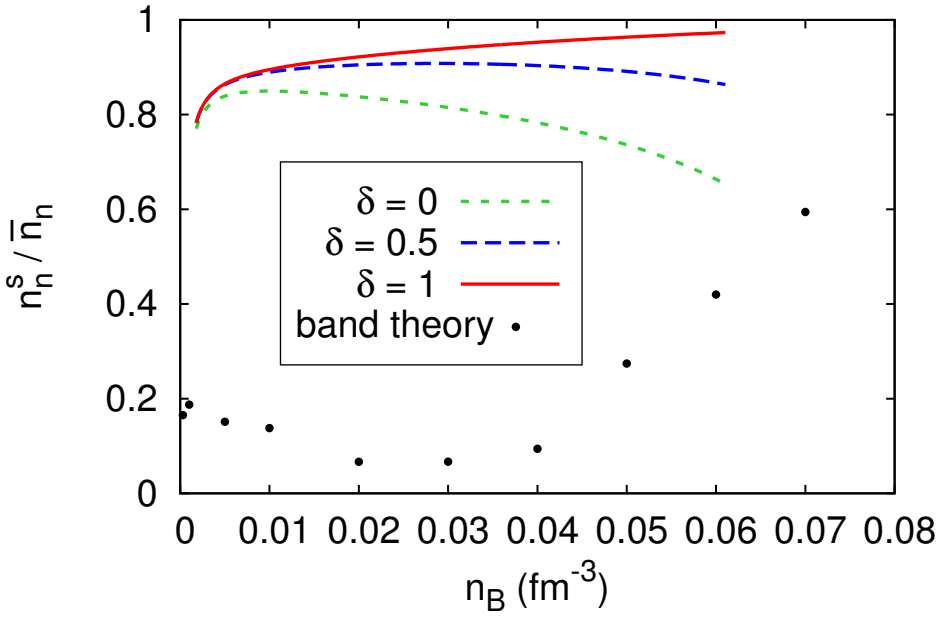

Martin&Urban,PRC94, 065801 (2016)
Magierski&Bulgac,Act.Phys.Pol.B35,1203(2004); Magierski, IJMPE13, 371(2004)
Sedrakian, Astrophys.Spa.Sci.236, 267(1996); Epstein, ApJ333, 880 (1988)

However, the assumption of strong pairing is usually not satified.

Suppression of band structure effects by pairing?

The role of pairing has been recently studied by Watanabe&Pethick by solving numerically the HFB equations at $\bar{n} = 0.03$ fm^{-3}.
But approximations were made:

- 3D body-centered cubic lattice replaced by a **1D lattice**
- $B(\boldsymbol{r}) = \hbar^2/(2m_n)$
- **Fourier components of $U(\boldsymbol{r})$ contribute independently**

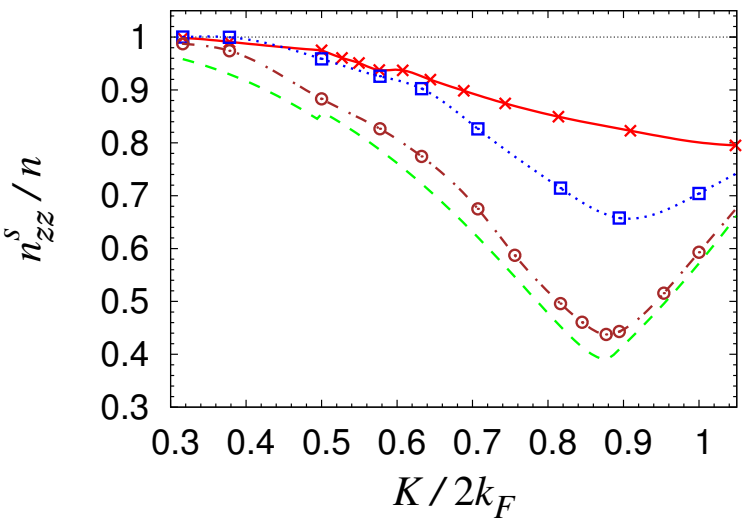

$$V_{\rm ext}(z) = 2V_K \cos(Kz)$$
$$V_K = 0.25(K/2k_F)^2\varepsilon_F$$

green dashed: no pairing
brown dashed-dotted: $\Delta = 0.0464\varepsilon_F$
blue dotted: $\Delta = 0.208\varepsilon_F$
red solid: $\Delta = 0.686\varepsilon_F$

Watanabe&Pethick,PRL119,062701(2017)

For realistic pairing gaps $\Delta \sim 1 - 1.5$ MeV, $n_n^s/n_n^f \sim 60 - 70\%$.

Role of pairing further examined

- full **3D band-structure** calculations (body-centered cubic lattice)
- same potentials $B(\boldsymbol{r})$ and $U(\boldsymbol{r})$ as those employed in 2012
- pairing included in the **BCS approximation**

$$n_n^s = \frac{m_n}{24\pi^3\hbar^2}\sum_\alpha \int |\nabla_{\boldsymbol{k}}\varepsilon_{\alpha\boldsymbol{k}}|^2 \frac{\Delta^3}{E_{\alpha\boldsymbol{k}}^3} \mathrm{d}^3k \qquad E_{\alpha\boldsymbol{k}} = \sqrt{(\varepsilon_{\alpha\boldsymbol{k}}-\mu)^2+\Delta^2}$$

Whole range of Δ considered up to largest possible values:

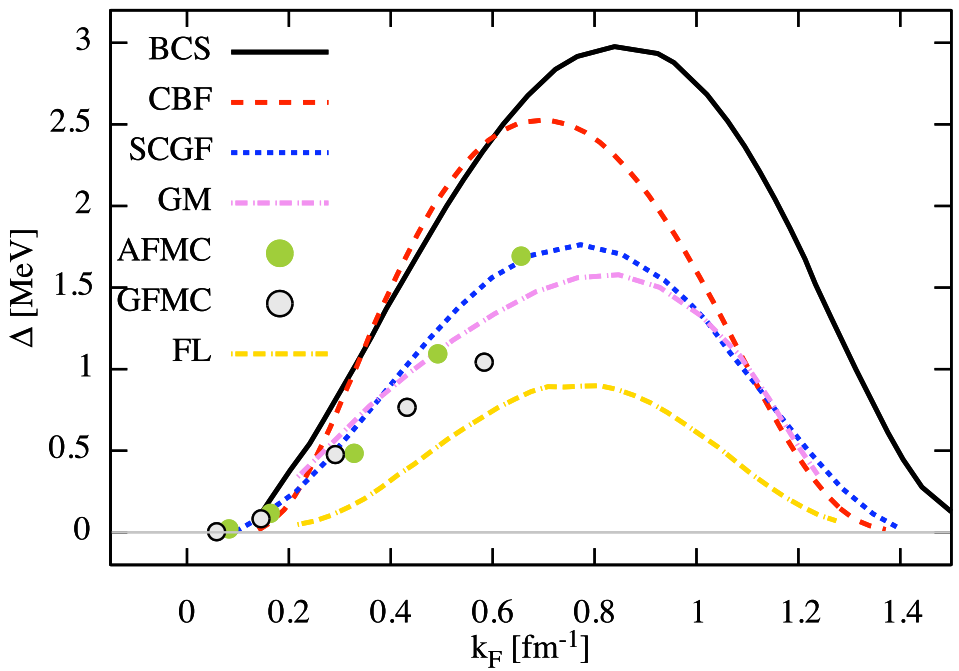

Adapted from Sedrakian&Clark, arXiv:1802.00017

Role of pairing further examined

- full **3D band-structure** calculations (body-centered cubic lattice)
- same potentials $B(\boldsymbol{r})$ and $U(\boldsymbol{r})$ as those employed in 2012
- pairing included in the **BCS approximation**

Δ (MeV)	$\Delta/\varepsilon_{\rm F}$	n_n^s/n_n^f (%)
3.09	0.169	7.87
2.16	0.118	7.74
1.51	0.0826	7.63
1.06	0.0578	7.56
0.741	0.0405	7.55
0.519	0.0283	7.57
0.363	0.0198	7.61
0.254	0.0139	7.66
0.178	0.00972	7.77
0.125	0.00680	7.76
0	0	7.84

Results obtained using a new computer code based on a FFT grid of $25 \times 25 \times 25$ points with up to 1650 bands.

Brillouin zone integrations performed using up to 65280 points.

Chamel, in prep.

Including pairing is computationally very costly, but results are essentially the same as those obtained without.

Role of quantum zero point motion and pairing

Kobyakov&Pethick speculated that entrainment could be suppressed by quantum zero-point motion of ions about their equilibrium position.

Kobyakov&Pethick, Phys. Rev. C 87, 055803 (2013)

Δ (MeV)	n_n^s/n_n^f (%)
3.09	8.24
2.16	8.07
1.51	7.95
1.06	7.88
0.741	7.87
0.519	7.89
0.363	7.93
0.254	7.98
0.178	8.01
0.125	8.04
0	8.10

Results of **3D band-structure calculations** accounting for quantum zero-point motion of ions via the **Debye-Waller factor using bare ion mass** M.

Entrainment is actually enhanced!

Chamel, in prep.

Quantum zero-point motion of ions is found to be small, and in reality is suppressed by entrainment ($M^\star > M$).

All in all, superfluid neutrons are still strongly entrained by the crust.

Conclusions I

We have calculated the equation of state of neutron-star crusts using the density functional theory

- varying the neutron-matter stiffness (BSk19-21) & symmetry energy (BSk22-26)
- considering catalyzed, highly-magnetized and accreted crusts.

The same functionals have been used to determine the equation of state of neutron-star cores thus providing a unified description.

Analytical fits:
(including composition & local nucleon distributions)
`http://www.ioffe.ru/astro/NSG/BSk/`

Perspectives:

- Extension to finite temperatures (neutron-star mergers),
- Go beyond the single-nucleus approximation,
- Allowance for nuclear “pasta” mantle (if any) beneath the crust,

Conclusions II

- **Superfluid neutrons in neutron-star crusts do not flow freely** similarly to superfluid ^{4}He on thin films, superconducting electrons in solids, or atomic gases in optical lattices.
- **3D band-structure calculations** show that neither pairing nor quantum zero-point motion of ions can suppress entrainment.
- Entrainment is found to be the strongest ($n_n^s \lesssim 10\% n_n^f$) at densities $\sim 0.02 - 0.04$ fm^{-3}.

Perspectives:

- Systematic calculations of n_n^s using more recent neutron-star crust models
- Extension to finite temperatures
- Role of the spatial arrangement of clusters (disorder)